Application of high-speed imaging to determine the dynamics of billiards

S. Mathavan,[a] M. R. Jackson,[b] and R. M. Parkin[c]
Mechatronics Research Group, Wolfson School of Mechanical and Manufacturing Engineering, Loughborough University, Loughborough LE11 3UZ, United Kingdom

(Received 19 December 2008; accepted 2 June 2009)

In spite of interest in the dynamics of the billiards family of games (for example, pool and snooker), experiments using present-day inexpensive and easily accessible cameras have not been reported. We use a single high-speed camera and image processing techniques to track the trajectory of snooker balls to 1 mm accuracy. Successive ball positions are used to measure the dynamical parameters involved in snooker. Values for the rolling and the sliding coefficients of friction were found. The cushion-ball impact was studied for impacts perpendicular to the cushion. The separation angles and separation velocities after an oblique collision were measured and compared with predicted values. Our measurement technique is a simple, reliable, fast, and nonintrusive method, which can be used to test the numerous theories for the dynamics of billiards. The addition of a spin tracking element would further broaden its capabilities. © *2009 American Association of Physics Teachers.*
[DOI: 10.1119/1.3157159]

I. INTRODUCTION

Pool and snooker are popular billiard games. Billiard games involve very subtle physics and have been of interest to the physics community for over 200 years. The first extensive treatment of billiards was by Coriolis in 1835.[1] Other works, such as those of Wallace and Schroeder,[2] Salazar and Sanchez-Lavega,[3] and de la Torre Juárez,[4] address the dynamics of billiards. There have been both theory and experimental works[5] on the dynamics.

Special apparatus have been used for the measurements in most instances. For example, glass and textured black formica was used to replace the table-felt in studying the collisions between billiard balls.[2,5] Tracking techniques such as spreading talcum powder on the surface of the table have also been employed. Many of these techniques affect the dynamics that is being studied. Although Bayes and Scott[5] used a Polaroid camera and a stroboscope to track the balls, they did not base their results on this setup probably due to the poor accuracy of the cameras in the 1960s. As recent as 1994, rudimentary techniques were still used to estimate the physical parameters in billiard dynamics. For example, Marlow[6] used a meter stick and a stop watch to measure friction coefficients.

Today's technologies allow the high resolution tracking of objects. High-speed tracking technologies are extensively used in sports such as football, tennis, and cricket.[7,8] Alciatore[9] used high-speed video capture to visualize the dynamics in the game of pool. Alciatore[10] also used infrared imaging to visualize the collision points. However, he did not analyze the images to extract the physical parameters involved in the dynamics. Cross[11] employed a video camera to measure the ball velocity and ball spin using an overhead camera and analyzed squirt dynamics in a cue ball suspended as a pendulum bob. Researchers involved in robotic billiards have also used overhead cameras to locate the static ball positions on the table.[12–15]

In this paper we use high-speed camera based tracking to measure the characteristics of the interactions between the cue ball, table, and object ball. Accurate spatial and temporal tracking of the ball and the use of speed-time plot of the balls allow us to distinguish the different phases of ball dynamics, such as sliding, rolling, and impulses. The accurate detection of the changes in the phases of the ball motion allows us to measure the parameters more accurately than has been done. The use of speed-time plots also allows us to measure the effects of special collision between two balls, such as "overspinning," which has only been qualitatively described in the literature.

II. EXPERIMENTAL SETUP

A Riley Renaissance type snooker table with dimensions of 10×5 ft^2 was installed in our laboratory (see Fig. 1). This brand is the official table of the World Snooker Association and has been used for its professional snooker tournaments since 1992.

The tables used in pool and snooker are almost identical, except that the pool table has larger pockets compared to the size of a pool ball. At the start of a game there are 21 colored balls worth various points and a white cue ball at predefined places on the table.

A machine vision camera was mounted on the ceiling, right above the snooker table, looking vertically downward (Fig. 1). A single camera is sufficient to capture the dynamics because the dynamics is confined to the table surface. The color camera is PixeLINK PL-B776F with 3.15×10^6 pixel resolution. The camera is connected to a host personal computer via FIREWIRE. For the region of interest option the camera is capable of capturing up to 1000 frames per second (fps). This feature of the camera was used whenever it was necessary to analyze the dynamics at finer temporal resolutions. The camera is fitted with a wide-angle lens to capture the whole table from the limited available headspace between the snooker table and the ceiling. The table area is imaged to a 1 mm spatial resolution with the current setup of the camera.

To verify that the measurements made by the camera are accurate, some distance measurements were also made with a meter stick. For this purpose two rectangular blocks with a height of the ball radius and with circular white patterns on their top surfaces were placed at two locations on the table. Circular patterns of diameter of 52.4 mm (the ball diameter) were used so that the camera and the image processing algorithm would treat them as balls. The distance between their centers was obtained using the camera and the meter stick.

Fig. 1. Snooker table and ceiling-mounted machine vision camera in the mechatronics laboratory. Note the headspace and the vertical mount of the camera to look perpendicularly down at the table.

We used this method because it was very cumbersome to physically measure the center distance between two snooker balls because the balls change position with the slightest touch. This procedure was repeated for several random positions of the blocks almost covering the whole imaged area of the table. The differences in the measurements by the two methods were found to be at most 2 mm, validating the results from the imaging system. The video and image handling and the image processing were performed using MATLAB.

A. Methods

Before measurements could be made on the images from a camera, two calibrations were done. The intrinsic camera calibration was performed to correct for the lens distortion that is present in wide-angle lenses [see Fig. 2(a)]. The camera calibration toolbox from the Computational Vision Group at Caltech was used in conjunction with MATLAB to calibrate the camera; for a detailed description of the procedure, see Ref. 16.

The MATLAB toolbox also incorporates an extrinsic calibration element. The extrinsic calibration procedure enables metric measurements to be made from the values given in terms of pixels. This procedure provides the translation and rotation matrices that relate the real world coordinate system to the image plane (see Fig. 3). The equation for the transformation between a point in the world frame xyz to its corresponding image point in the camera fame $x'y'z'$ is $x'=Rc^{*}x+Tc$, where Rc and Tc are the rotation and translation matrices, respectively.[17]

A real world coordinate system was selected such that it was fixed to the snooker table so that two of its axes lie along the two perpendicular edges of the table and both x and y lie on the imaginary plane that is created by the ball centers [see Fig. 2(b)], which is 26.2 mm above the table surface. The

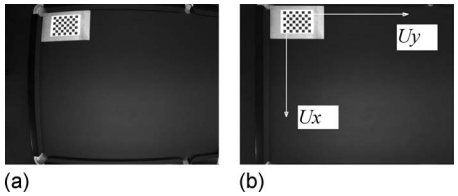

Fig. 2. (a) Distorted and (b) corrected images of the half table (note the barrel distortion due to the wide-angle lens) with the checkerboard pattern, for extrinsic camera calibration, placed on the table.

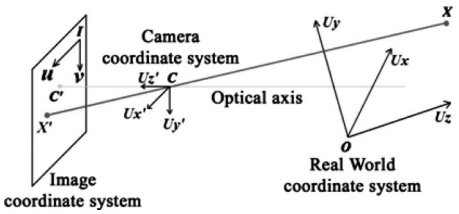

Fig. 3. The pinhole camera model shows how a real world point X is projected as X' on the camera image plane uv, through the optical center C of the lens. Also note how the camera frame $x'y'z'$ is fixed to the optical center of the lens.

experiments were performed in half of the table area to obtain better spatial resolution from the camera. The image blur due to fast moving balls was minimized by selecting the lowest possible camera shutter opening time. Image sequences with high image blurs were not analyzed. Quantification was done by counting the number of pixels in a blur and then comparing it with the number of pixels found in a stationary ball.

B. Image processing

An image processing program was written to execute the following operations. The video was captured and then split into image frames. The images were then converted into gray scale images. Each of these gray scale images were then transformed to binary images using an appropriate threshold value of the image intensity. A treatment of these concepts can be found in textbooks on digital image processing such as that of Gonzalez and Woods.[18] Then the image processing program to extract the ball centroid was executed. Two functions from the MATLAB Image Processing Toolbox called *bwlabel* and *regionprops* were used to extract the ball from the image, thus determining its centroid in pixels. The real world coordinates of the ball centroid are obtained using the transformation matrices Rc and Tc from the extrinsic calibration procedure. The time stamping of these values based on the camera frame rate enables us to calculate the velocities and accelerations of the ball.

III. RESULTS AND DISCUSSION

The tracked cue ball is shown with its initial position on the snooker table in Fig. 4. The spatial separation between the successive tracked centroids indicates the variation in the ball's velocity.

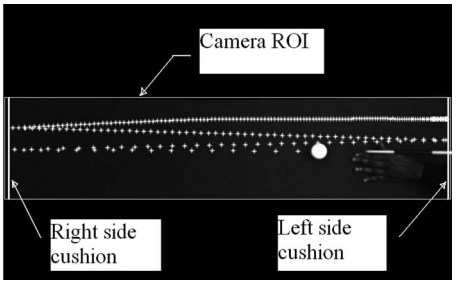

Fig. 4. The tracked cue ball positions (the centroid of the ball is shown by the white markers) are superimposed on the image at the start of the tracking, also showing the initial cue ball location (four consecutive impacts with two parallel cushions are shown).

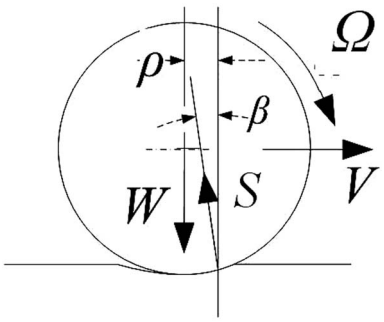

Fig. 5. The ball rolling on the table. It shows the forces that are acting on the ball while it is rolling. Note the reaction force from the table S, which is a combined effect of the "regular" normal reaction from the table and, most importantly, due to of the table-felt under the weight of the moving ball. The horizontal component of S, $S \sin \beta$, decelerates the ball.

A. Ball motion against surface friction on the table

When there is no relative velocity between the ball and the table at their contact point, the ball is said to roll on the table. During the rolling the linear and angular velocities of the ball, V and Ω, respectively, satisfy the relation $V=R\Omega$, with R the ball radius. Because the table-felt is deformable and the ball is rigid, the table surface deforms when the ball is in motion as shown in Fig. 5. Hence the ball makes contact with the table over an extended area. According to Ref. 19 this deformation is independent of V. The table cloth deformation results in a normal reaction force S from the table at an angle β with the vertical, inclined from the moving direction of the ball as shown in Fig. 5. For an extensive treatment of this deformation, see Refs. 19 and 20.

According to Fig. 5, the reaction force S has a horizontal component equal to $S \sin \beta$, which opposes the ball motion. Generally the reaction force S does not go through the centroid of the ball, and hence there is a torque acting in the opposite direction to that of the angular velocity Ω, resulting in angular deceleration. The rolling friction coefficient does not change with the ball's velocity and is a constant because it depends only on the surface properties of the table-felt and the geometry and mass of the ball.[19]

Figure 6 shows the variation in the ball's velocity with respect to time. Once the impulse is delivered to the ball, the ball's velocity decreases rapidly during what is known as the sliding phase, and then the ball starts to roll. Reference 3 showed that the ball starts to roll immediately only when the ball is hit horizontally at a height of $7R/5$ from the table surface. In Fig. 6 the velocity gradient during the rolling phase gives the value of the deceleration due to rolling friction. Different shots were tracked and the deceleration during the rolling phase was found to be 0.124–0.126 $\mathrm{m/s^2}$. The rolling friction coefficient, which is usually expressed as a fraction of the gravitational acceleration 9.81 $\mathrm{m/s^2}$, is 0.0127–0.0129. Marlow[6] suggested a range of 0.011–0.024 for pocket billiards (pool) and a mean value of 0.016. Although the physical properties of the ball and table are different in pool and snooker, there is no obvious reason for this excessive variation (more than 100% of the lower value) obtained in pool with Marlow's measurements. The only plausible explanation is that the meter stick and stop watch measurement method used by Marlow is prone to error. Although Williams[21] claimed that the nap of the table-felt affects the ball motion, depending on whether its motion is toward the top cushion or away from it, we did not find any evidence to support this claim.

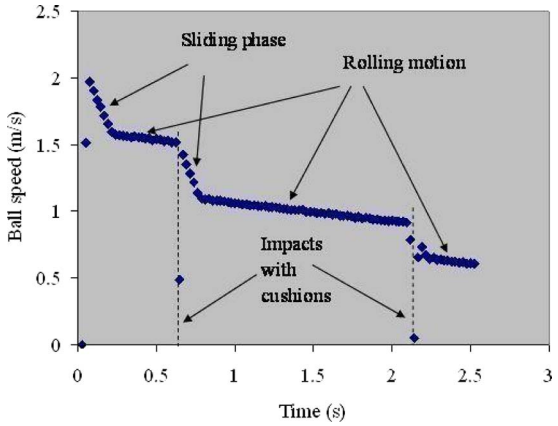

Fig. 6. The speed-time plot for the ball showing all the different phenomena involved from the video captured at 42 fps (the complete motion profile until the ball comes to the rest is not shown here).

When there is a relative velocity between the ball and the table at their point of contact, the ball is said to slip on the table. In the sliding phase $V=R\Omega$. For a theoretical treatment of all the possible cases of ball motion immediately after the cue impact, see Ref. 3. The friction that exists during the sliding motion (the sliding coefficient of friction) usually depends on the sliding velocity of the ball. The ball speed-time plot given in Fig. 6 shows that the sliding friction is much larger than the rolling friction, disappears within a very short time interval, and quickly diminishes with the velocity. Another interesting observation from this plot is that after the ball has started its rolling motion, it starts to slide again (note the speed gradients immediately after the impacts) when it collides with the cushion (table wall/rail) because the cushion impact violates the $V=R\Omega$ rolling condition. Once $V=R\Omega$ is reached again, the ball goes into the pure rolling mode.

From the analysis of the speed of the tracked ball, the sliding friction coefficient was found to be in the range of 1.75–2.40 $\mathrm{m/s^2}$ (0.178–0.245 in dimensionless units). These values were obtained for the ball motion along random directions on the table. Marlow[6] calculated a dimensionless value of 0.2 for pool using the rolling coefficient value of 0.016. An independent measurement was not performed because only a meter stick and a stop watch were available. Witters and Duymelinck[22] used stroboscopic illumination to photograph a decelerating pool (not snooker) ball. They found that when the ball velocity increases from zero, the friction coefficient approaches 0.21 from a value of 0.14. Such a variation could not be verified from our experiments.

The sliding friction is 15–20 times larger than the rolling friction. Also, during the sliding phase some rolling action will simultaneously take place, as the displacement effect, shown in Fig. 5, is always present at the ball-table interface. Due to its comparatively small magnitude (approximately 5%), it is usually neglected, and the motion is treated as pure sliding.

B. Ball-cushion interaction

To visualize and analyze the impulse dynamics between the ball and the cushion, high-speed image capturing experi-

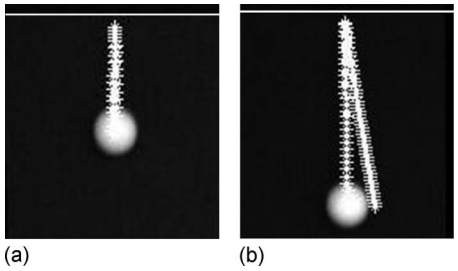

Fig. 7. Bounce of the cue ball off the rail. The ball location depicts its position as it approached the rail. The frame rate is 120 fps, and an imaginary continuous white line shows the approximate location of the cushion.

ments with >100 fps for small regions of interest were performed. The impulse of the cue ball on the cushion depends on factors such as the speed at which it collides with the cushion surface, the incident angle with respect to the cushion surface, the amount of spin of the ball, the physical characteristics of the ball and the cushion, and the parameters involved in the interaction between the ball and the cushion such as the coefficient of restitution and the surface friction.

Spin on the ball changes the impact characteristics drastically. Ball spin is difficult to quantify with our experimental setup and methodology. Sidespin changes the postimpulse cue ball path significantly; the interested reader is directed to Ref. 23 or Ref. 9. The ball-cushion interaction is a case of multiple impacts, both normal and tangential, the latter due to the force of friction, with one component normal to the cushion surface, and the other two perpendicular frictional impacts from the cushion wall. Derivations of the dynamics for general impact are not available.

For this reason we conducted experiments on shots without considerable sidespin. Care was taken so that a shot was directed perpendicular to the rails (cushions) as much as possible. Whenever the cue ball is played perpendicular to the rails, if it does not have any sidespin and should bounce back along the same path along which it approached the rail. This criterion was used to ensure that the shots did not impart a considerable sidespin on the cue ball. Figure 7(a) shows a perpendicular shot with no sidespin, and Fig. 7(b) shows a perpendicular incoming shot that apparently has some sidespin, which results in the ball rebounding to the right side. For the rebound analysis the shot shown in Fig. 7(b) was not used, and only the one shown in Fig. 7(a) was used. The no-sidespin condition ensures that there is only one unknown in the form of top/back spin.

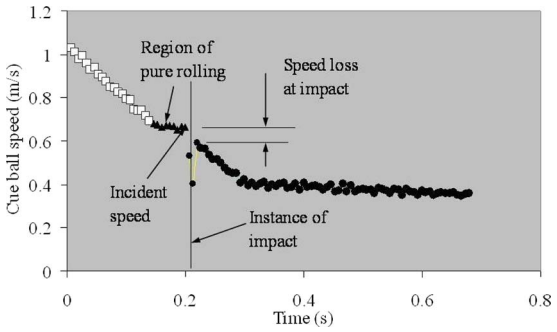

Fig. 8. The tracked results for a ball-cushion impulse (at 150 fps).

If we assume that the ball had gone into pure rolling mode before the impact, we can determine the top spin of the ball from $\Omega = V/R$. Thus the incident ball velocity V is the only independent variable involved, and the velocity drop during the impact can be correlated with V.

Figure 8 shows the velocity plot obtained from a high-speed video captured at 150 fps. The velocity plot was used to determine if the ball was rolling just before it hit the cushion. The gradient of the speed-time plot was used to determine this, as shown in Fig. 8. Results that were obtained for 31 such shots into the rails, almost satisfying the conditions of no-sidespin and that of pure rolling, are given in Fig. 9.

From Fig. 9 we see that the relation between the rebound and incident speeds is almost linear for the incident velocity in the range of 0.28–3.5 m/s (the typical range of ball velocities in the game). A best fit straight line for the rebound-incident speed data gives a coefficient of restitution of 0.818 for this velocity range. The results are more closely fit by the second-order polynomial $y = -0.0877x^2 + 1.131x - 0.0953$, where x is the incident velocity and y is the rebound velocity. These results are not valid for a general ball-cushion impulse but are applicable only under the conditions of no-sidespin and pure rolling motion prior to the impulse. We believe that the ideal variation between the rebound and incident speeds should be linear and the reduction in the coefficient of restitution at higher incident speeds is due to cushion deformation. The gradient of the plot at lower incident speeds is around 0.910, and this value shall be valid under the assumption of a rigid cushion.

Marlow[6] reported that the coefficient of restitution for rails in a billiard table is 0.55 but did not give much detail about the experimental procedure. He compared his results with the values suggested by Coriolis[1] and concluded that they agree closely.[6] The cushion height for snooker is 36 mm, with the ball radius equal to 26 mm, which is close to the height of 1.4 times ball radius found in pool. Thus the cushion and ball geometry is almost identical in pool and snooker. It is possible that Marlow considered the rebound ball velocity at the end of the sliding phase rather than the correct one immediately after the impulse. Then the coefficient of restitution for the shot could be 0.63, but this result has no physical meaning.

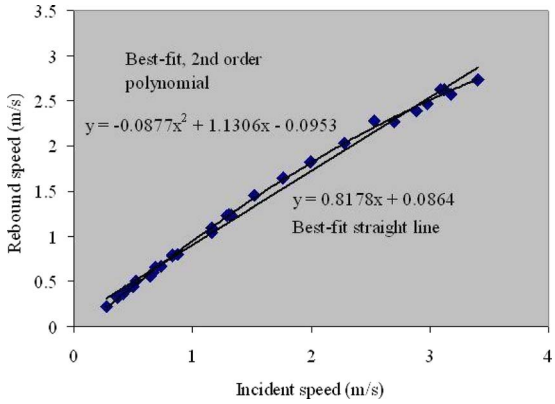

Fig. 9. The variation in the rebound velocity versus the incidence velocity. At lower incident velocities the variation is almost linear. However, at higher incident velocities the rebound velocities tend to level off, quite possibly as the cushion is not rigid at higher incident speeds.

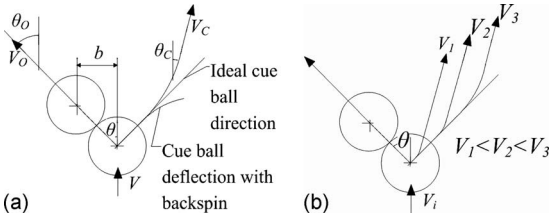

Fig. 10. The effect of table friction on the cue ball path for an oblique collision (from Ref. 2). (a) The parameters involved in an oblique collision. (b) The cue ball path for different precollision cue ball speeds under rolling conditions.

C. Impact between balls

If the approaching and separating velocities of two balls lie along the line connecting the centers of the balls, then the impact is said to be frontal or head-on. Impacts occur in two dimensions in billiards as oblique collisions, and the frontal impact is a special case.

Amateur billiards players use the 90° rule[9,10] to visualize the postcollision trajectories of the colliding balls. It states that the balls will separate at 90° after an oblique collision (see Fig. 10 for the predicted ideal directions of travels). It is also assumed that the cue ball will immediately stop after a frontal collision. In snooker the cue ball and all object balls have the same mass. It can be easily shown by momentum conservation that the 90° rule only holds when the coefficient of restitution between the balls is one (that is, the balls are purely elastic). The angular velocity of the cue ball (in the form of the side/top spin) when it collides with the object ball also affects the postcollision velocities and the directions of separation for the balls. The friction present between the colliding balls has also been shown to affect the postcollision motion.[24] Bayes and Scott[5] employed a spring loaded cue launcher and two pool balls on a felt-covered table to examine this effect. They used a stroboscope and a camera to determine the subsequent ball paths and found that the angle was around 67°. There is no data on how much spin the ball had at the time of impact, which is known to affect the collision dynamics. They also tested the ball on various glass surfaces and found that the collision angle approaches 90° as the surface becomes smoother (in soapy glass it reached 89.9°). Thus table friction creates some unpredictable behavior in the ball collision.

The tracked results for the cue ball and an object ball collision are shown in Fig. 11. We see that the temporal resolution of the tracking is sufficient to capture the deflections in its postimpact trajectory. The reason for the curvature in the path of the cue ball is that it starts to slip immediately after the impact [a similar slipping phenomenon was also observed in the ball collision with a cushion; see Fig. 10(a)]. Figure 10(b) gives an idea of how this behavior is influenced by the incident velocity of the cue ball. Similarly, the object ball also starts to slip immediately after the impact. Once the slipping phase has stopped, both balls go into rolling motion, and the curved path of the cue ball is then directed along the tangent line to the curve. Reference 2 analyzed this phenomenon and showed that the velocities for the postcollision and postsliding phases of the object ball are (see their notation in Fig. 10)

$$V_O = \tfrac{5}{7} V \cos\theta,$$

$$\theta_O = \theta, \tag{1}$$

and for the cue ball is

$$V_C = \tfrac{5}{7} V \sqrt{\tfrac{9}{5}\sin^2\theta + \tfrac{4}{25}},$$

$$\theta_C = \tan^{-1}\left[\frac{\sin\theta\cos\theta}{\left(\sin^2\theta + \frac{2}{5}\right)}\right]. \tag{2}$$

They defined $\beta = b/D$ as the fractional impact parameter, where D is the ball diameter and b is the separation of the ball centers in the direction perpendicular to the incident ball velocity V. Also note that $\beta = \sin\theta$.

Plots of angles θ_o, θ_c, and $\theta_o + \theta_c$ versus the impact parameter are shown in Fig. 12. The experimental values agree with the theoretical predictions in most instances, but θ_o deviates more from its theoretical value at high fractional impact values. The reason is unknown, and we do not know if factors such as spin affect collisions for very oblique collisions. A possible explanation is that at high values of b, an excessive amount of sidespin is imparted to the object ball, which changes its path from what is derived in Ref. 2. This phenomenon also raises questions about whether sidespin affects its speed or direction of travel.

In billiards sidespin is considered to be independent of the linear speed of the ball because it is assumed that the ball makes a point contact with the table. If both the contacting surfaces are extremely rigid, this assumption would be valid. For billiards the rigid table-top is covered by a soft felt. Thus a considerably rigid billiard ball sinks into the felt, making contact over a finite region of the ball's surface. Hence we suspect that the ball exhibits disklike properties. For a flat disk, such as an ice-hockey puck, its linear motion and its

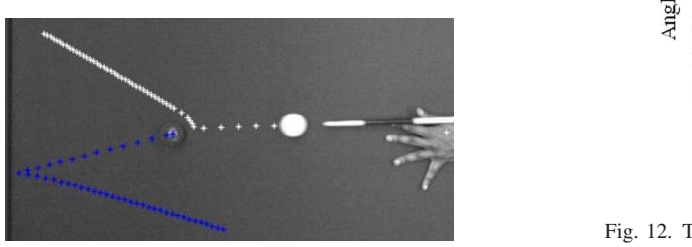

Fig. 11. Tracking results for a collision between the cue ball and an object ball at 45 fps.

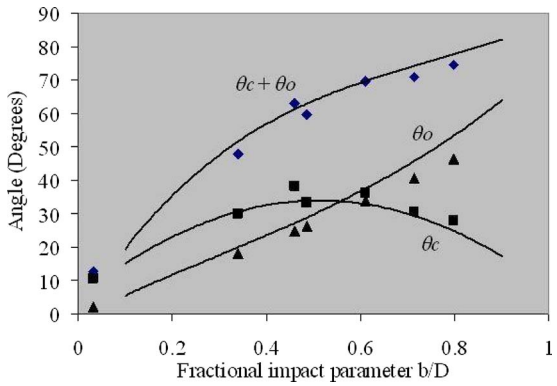

Fig. 12. Theoretical and measured deflection angles for the cue and object balls versus the fractional impact parameter β. The symbols ■, ▲, and ◆ represent θ_c, θ_o, and $\theta_c + \theta_o$, respectively. Continuous lines show the respective predictions.

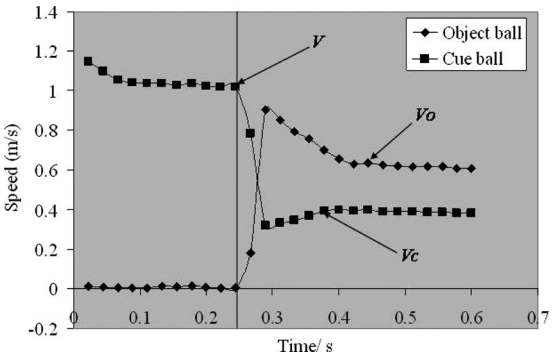

Fig. 13. A typical speed variation in the cue ball and object ball near impact. It shows how both the cue ball and the object ball start to slip on the table immediately after their collision. The cue ball speed plot also shows how the cue ball is accelerated after the impact.

rotation (it only has a side-rotation, which is analogous to the sidespin of the ball) are always coupled.[25] That is, the rotational motion and linear motion of a disk will end at exactly the same time.[25] Thus there are some characteristics of the disklike motion found in billiard ball motion. One observation that supports this claim is that we never see the ball continue to rotate about the vertical axis (that is, sidespin) after its linear motion is stopped. The coupling of linear and rotational motions is readily apparent in the game of pool where the balls have a number or other pattern painted on their surface.

Wallace and Schroeder[2] did not experimentally validate the velocity relations found in Eqs. (1) and (2) because their tracking method could record only the positions and not the time stampings. We use the velocity plots for both colliding balls to validate these equations. As shown in Fig. 13, the incident velocity is measured right at impact. The gradient, typical for the pure rolling motion, as discussed, was used as the criteria for detecting the time at which the ball starts to roll (or stops slipping). The detected times are shown with their respective velocity symbols in Fig. 13. We observe that the cue ball accelerates right after the collision. This acceleration occurs because the collision greatly reduces only the linear velocity and not the angular velocity, and thus the cue ball goes into a sliding condition with excess top spin (overspinning). This excess top spin is then converted into linear velocity by the action of the sliding force, which in this case acts in the same direction as the ball velocity, increasing the latter.

The results are given in Table I for five such shots involving impacts. The maximum error between the theory and the measurements is found to be around 10%. We do not know whether this error is also induced by the effect of sidespin on the collision between two balls. The sidespin of the ball was not taken into consideration in Ref. 2. There is reason to believe that the friction between the cue ball and the object ball will introduce tangential force components at the collision point, which would impart a sidespin onto the object ball, even though the values of these tangential force components may be small.

During impulse there will be a relative velocity between the cue ball and object ball along the vertical due to the angular velocity (top spin) in the natural roll of the cue ball prior to the impact. This relative velocity will introduce a tangential friction force during the time of impulse on the cue ball as well as on the object ball. This force will induce a spin on the cue ball about its frontal velocity axis, producing an effect equivalent to a massé shot (a shot played with an elevated cue stick). For a massé shot a ball is known to move along a curved path instead of on a straight line. This correction should also be added to the prediction in Ref. 2. These observations and the evidence presented in Fig. 12 and Table I should motivate a new theory for the collision between two balls, which involves the frictional forces between the balls that are present during the impulse.

IV. CONCLUSIONS

High-speed video capture using a single machine vision camera was found to give good results in determining the dynamics involved in snooker. The rolling coefficient of friction was found to be between 0.124 and 0.126 m/s^2. The sliding friction value is in the range of 1.75–2.40 m/s^2. One-dimensional ball-cushion collisions were also analyzed, and the mean coefficient of restitution was determined. Both frontal and oblique collisions between the balls were analyzed. Predictions of separation angles and velocities were tested experimentally and close agreement was found.

Some experiments could not be performed. One such experiment would look at the general impact of the ball with the cushion. The inability to perform such experiments is mainly due to the difficulty of determining the amount of spin on the ball using the camera. To track the ball spin in football and golf, researchers have used marked patterns on the ball surface. Some interferometer based techniques have also been used for this purpose.

Table I. The postimpact speed theoretical predictions (Ref. 2) and the measured values from ball tracking. V is the incoming cue ball speed, θ is the cut angle for oblique collision, V_o and θ_o are the postcollision and postslip direction of travel and speed for the object ball, and V_c and θ_c are the postcollision and postslip direction of travel and speed of the cue ball.

V (m/s)	θ (°)	Measured V_c (m/s)	Measured V_o (m/s)	Theoretical V_c (m/s)	Theoretical V_o (m/s)	Error in V_c (%)	Error in V_o (%)
1.539	33.83	0.816	0.836	0.932	0.913	12.4	8.43
1.032	26.36	0.520	0.629	0.529	0.660	1.70	4.70
1.364	40.52	0.925	0.700	0.934	0.740	0.964	5.40
1.731	46.50	1.275	0.787	1.301	0.851	2.00	7.52
0.942	18.05	0.365	0.581	0.388	0.640	5.93	9.22

ACKNOWLEDGMENTS

The authors are indebted to the anonymous reviewers for their insightful, critical, and enthusiastic comments that resulted in an improved manuscript.

[a]Electronic mail: s.mathavan@lboro.ac.uk
[b]Electronic mail: m.r.jackson@lboro.ac.uk
[c]Electronic mail: r.m.parkin@lboro.ac.uk

[1] G.-G. Coriolis, *Théorie Mathémathique des Effets du Jeu de Billard* (Carilian-Goeury, Paris, 1835) translated by David Nadler [*Mathematical Theory of Spin, Friction, and Collision in the Game of Billiards* (David Nadler, USA, 2005)].
[2] R. E. Wallace and M. C. Schroeder, "Analysis of billiard ball collisions in two dimensions," Am. J. Phys. **56** (9), 815–819 (1988).
[3] A. Salazar and A. Sanchez-Lavega, "Motion of a ball on a rough horizontal surface after being struck by a tapering rod," Eur. J. Phys. **11**, 228–232 (1990).
[4] M. de la Torre Juárez, "The effect of impulsive forces on a system with friction: the example of the billiard game," Eur. J. Phys. **15** (4), 184–190 (1994).
[5] J. H. Bayes and W. T. Scott, "Billiard-ball collision experiment," Am. J. Phys. **3** (31), 197–200 (1962).
[6] W. C. Marlow, *The Physics of Pocket Billiards* (MAST, Palm Beach Gardens, FL, 1994).
[7] G. Pingali, A. Opalach, and Y. Jean, "Ball tracking and virtual replays for innovative tennis broadcasts," in Proceedings of the 15th International Conference on Pattern Recognition, Barcelona, Spain, 2000, Vol. 4, pp. 152–156.
[8] K. Davis, "A watchful eye" (www.matrox.com/imaging/news_events/feature/archives/2002/hawkeye.cfm).
[9] D. G. Alciatore, *The Illustrated Principles of Pool and Billiards* (Sterling, New York, 2004).
[10] D. G. Alciatore, "Pool and billiards physics principles by Coriolis and others" (http:billiards.colostate.edu/physics/Alciatore_AJP_MS22090_revised_pool_physics_article.pdf).
[11] R. Cross, "Cue and ball deflection (or "squirt") in billiards," Am. J. Phys. **76** (3), 205–212 (2008).
[12] F. Long, J. Herland, M.-C. Tessier, D. Naulls, A. Roth, G. Roth, and M. Greenspan, "Robotic pool: An experiment in automatic potting," in Proceedings of the IEEE/RSJ International Conference on Intelligent Robots and Systems, Sendai, Japan, 2004, pp. 2520–2525.
[13] A. W. Moore, D. J. Hill, and M. P. Johnson, "An empirical investigation of brute force to choose features, smoothers and function approximators," in *Computational Learning Theory and Natural Learning Systems 3: Selecting Good Models* (MIT, Cambridge , MA, 1995), pp. 361–379.
[14] S. W. Shu, "Automating skills using a robot snooker player," Ph.D. thesis, University of Bristol, 1994.
[15] M. E. Alian, S. E. Shouraki, M. T. M. Shalmani, P. Karimian, and P. Sabzmeydani, "Roboshark: A gantry pool player," 35th International Symposium on Robotics, Paris, France (2004) (www.cs.sfu.ca/~psabzmey/personal/publ/papers/alian_roboshark_isr04.pdf).
[16] J. Y. Bouguet, Camera calibration toolbox for MATLAB (www.vision.caltech.edu/bouguetj).
[17] J. Heikkilä and O. Silvén, "A four-step camera calibration procedure with implicit image correction," in Proceedings of the IEEE Computer Society Conference on Computer Vision and Pattern Recognition (CVPR'97), San Juan, Puerto Rico, 1997, pp. 1106–1112.
[18] R. C. Gonzalez and R. E. Woods, *Digital Image Processing* (Prentice-Hall, Upper Saddle River, NJ, 2002).
[19] J. Hierrezuelo and C. Carnero, "Sliding and rolling: The physics of a rolling ball," Phys. Educ. **30** (3), 177–182 (1995).
[20] A. Domenech, T. Domenech, and J. Cebrian, "Introduction to the study of rolling friction," Am. J. Phys. **55** (3), 231–235 (1987).
[21] K. Williams, *Know the Game: Snooker*, 3rd ed. (A&C Black, London, 2002).
[22] J. Witters and D. Duymelinck, "Rolling and sliding resistive forces on balls moving on flat surface," Am. J. Phys. **54** (1), 80–83 (1986).
[23] J. Walker, "The physics of the follow, the draw and the massé (in billiards and pool)," Sci. Am. **249** (1), 124–129 (1983).
[24] A. Domenech and E. Casasus, "Frontal impact of rolling spheres," Phys. Educ. **26** (3), 186–189 (1991).
[25] K. Voyenli and E. Eriksen, "On the motion of an ice hockey puck," Am. J. Phys. **53** (12), 1149–1153 (1985).